JET–P(98)13

Safety Analysis of Water Cooled Components inside the JET Thermonuclear Fusion Tokamak

P Ageladarakis, N P O'Dowd[1], S Papastergiou, G A Webster[1].

JET Joint Undertaking, Abingdon, Oxfordshire, OX14 3EA,
[1]Imperial College, Exhibition Road, SW7 2BX, London, UK.

Preprint of a paper to be submitted for publication in
American Nuclear Society (ANS) Transactions, USA.

April 1998

ABSTRACT

The transient thermal behaviour of a number of components, installed in the vessel of the world's largest Fusion Tokamak (JET) has been examined with a theoretical model, which simulated normal operational conditions and abnormal scenarios namely: Loss of Coolant Flow; Loss of Torus Vacuum; and combinations. A number of theoretical results related to water and cryogenically cooled devices have been validated by a comprehensive experimental campaign conducted both inside the JET plasma chamber and in a test rig. The performance of water cooled components which may be subjected to boiling or freeze-up risks in case of a Loss of Water Flow event has also been analysed. Time constants of transient temperature changes were determined by the model while protective actions were prescribed in order to safeguard the equipment against associated risks. A completely automatic safety protection system has been designed on the basis of these analyses and implemented in the routine JET operation.

During operation of JET the safety code reacted several times within the specified time limits and protected the relevant components during real off-normal events.

Keywords: JET, fusion, Tokamak, safety, in-vessel component, freeze-up, boiling.

ABREVIATIONS

JET	Joint European Torus
MK1,2	Mark 1,2 Divertor
CFC	Carbon Fibre Composite
GN	Gaseous Nitrogen

INTRODUCTION

Safety of nuclear power plants is always a very important issue and for thermonuclear fusion devices it is strongly related to their future success and development. Aspects of safety have been analysed thoroughly in the literature [1]-[8], for this reason. There are in general two levels of concern. One which evolves around the risk to public health and a second which focuses on the potential damage to the plant. Damage to a future nuclear fusion plant may result from events unrelated to plant operation (eg earthquakes, aircraft impacts) or by an equipment and/or operation failure. In studies of fusion reactor safety (eg [6]) the former type of phenomena are allocated a low but finite probability and safety is assessed against Beyond Design Basis Accidents (BDBAs). The assessment of these risks is performed to see that a severe BDBA would not give rise to eg: a necessity to evacuate the general population. Such BDBA's are not, in general relevant to the present generation of research Tokamaks. Instead we are largely concerned with Design Basis Accidents (DBAs) [9], [10] caused by equipment or operational failure. The latter can be thoroughly analysed and their serious consequences avoided. Such analyses, applied to present Tokamaks, can be of use in future reactor design.

Plant damage may take place if significant stresses develop in the pipework of components when the coolant freezes or boils, during a total or partial loss of flow. In general, unacceptable temperatures and subsequent failure of structural components may occur during a number of operational transients caused by a power/cooling mismatch. Methods for quantifying and/or minimising the risk of plant damage have received far less attention than those involving a radiation release [11]-[13] although safety encompasses both topics equally.

The JET Tokamak (Figure 1) is the largest and most successful fusion facility in the world. Its overall height and diameter are 12m and 15m respectively. JET produced for the first time, a controlled fusion power in a Deuterium-Tritium (D-T) plasma of 1.7 MW for 2 s (1991), as well as a world record of 16.1 MW, with > 10 MW for 0.6 s (1997), both outstanding achievements in nuclear fusion. The JET Tokamak comprises a number of complex in-vessel structures which operate under stringent and sometimes conflicting requirements.

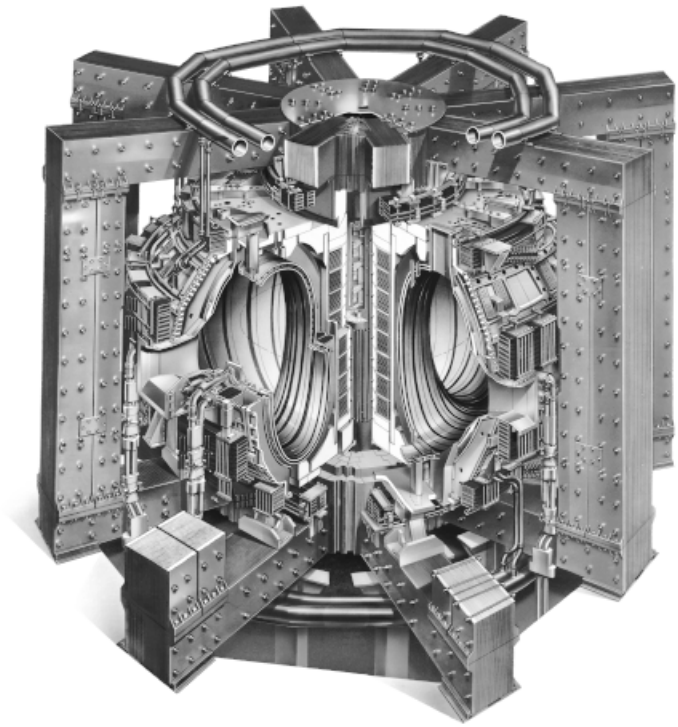

Figure 1. The JET Apparatus

Fusion reactions take place at temperatures in the order of 10^8 ^oC (100 times higher than the temperature of the centre of the sun). At these high temperatures the atomic structure of the reacting elements is that of a “plasma”, a fully ionised gas where electrons are stripped from the ions and move freely. The plasma is confined by high magnetic fields (4 Tesla) inside a toroidal-shaped vessel (4.1m high, 3.1m wide with 2.96m major radius) at ultra high vacuum levels (ie $>10^{-7}$ mbar). However, optimum plasma conditions can be sustained only for a few seconds, partly due to the adverse effect of plasma impurities in present fusion devices. Impurities result from the interaction between the outermost plasma trajectories and the vessel inner walls, separated by a distance of only a few cm. Continuous pumping of the majority of plasma

ions (D-T) and of impurities produces enhanced plasma performance and longer pulses [14], [15]. Active pumping capability at JET was achieved by a system of components placed at the bottom of the vessel, the so called Pumped Divertor, installed in 1994, at a total cost of £27 million.

The key water cooled elements of the Divertor Configuration are the target plates (plasma facing components) and the baffles, located underneath a long in-vessel helium condensation cryopump (Fig. 2). Both systems are individually cooled and in case of a loss of water flow event there is a potential risk of boiling or freezing due to continuous thermal flux or to the proximity of cryopump surfaces, respectively. Such developments must be avoided since they lead to relatively high stresses on the pipework.

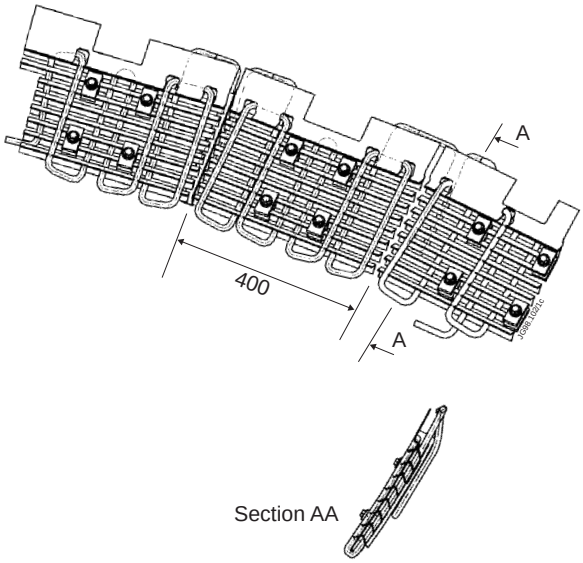

Figure 2. A section of the water cooled baffles of the JET Divertor.

1. GEOMETRY

1.1 Baffles

The baffles (Fig. 2) form a toroidal ring ~20 m long and 0.33 m high, which is tilted upwards by 24^{o} from the horizontal plane and is mounted at the bottom inner vessel wall, by telescopic bosses. They offer a thermal protection to the in-vessel cryopump (Fig. 3) and reduce the heat load from the relatively hot vessel by a factor of 20, to ~2.5 KW [16]. The baffles comprise a chevron type structure supported by the cooling circuit in a hair-pin arrangement. The 2 mm thick blackened chevrons are fabricated from a copper alloy (CuSiNi) and brazed on U-shape Inconel 600 pipes. Detailed information about the brazing techniques and material properties are found in [16], [17].

The whole assembly is divided into 8 subunits (octants) which are individually cooled by water at 5.5 bar and 20^{o}C. Every subunit consists of 2 sub-assemblies which

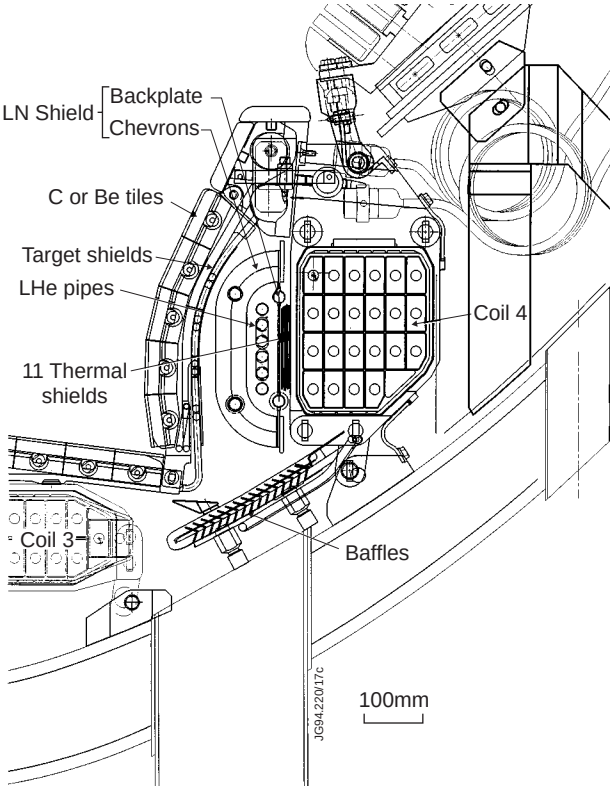

Figure 3. Cross section of the JET MK1 Divertor Cryopump System and its surrounding components.

weigh approximately 30 kg each. All in all, there are 8 parallel loops inside the vessel which merge eventually in one cooling circuit outside the vessel.

1.2 Target Plates (MK1 Divertor)

The target plates used in the JET experimental campaign of 1994-5 formed the so called MK1 Divertor, (Fig 4a). They featured three elements in a U-configuration, i.e., the horizontal and 2 vertical target plates. The target plates were grouped into 48 modules over their full toroidal length, with each module comprising eight elements. Similarly to the baffles, each module was cooled in a parallel arrangement from a single feed outside the torus.

Figure 5 gives a 3-dimensional view of a part of the side target plate. Solid tiles made from carbon fibre composite (CFC) or beryllium were attached, in pairs, onto water cooled support beams, made from stainless steel. The target plates carried 7296 tiles in total. The rows of tiles were separated by poloidal gaps, 10 cm wide, which allowed the transfer of plasma particles to the divertor cryopump area [18].

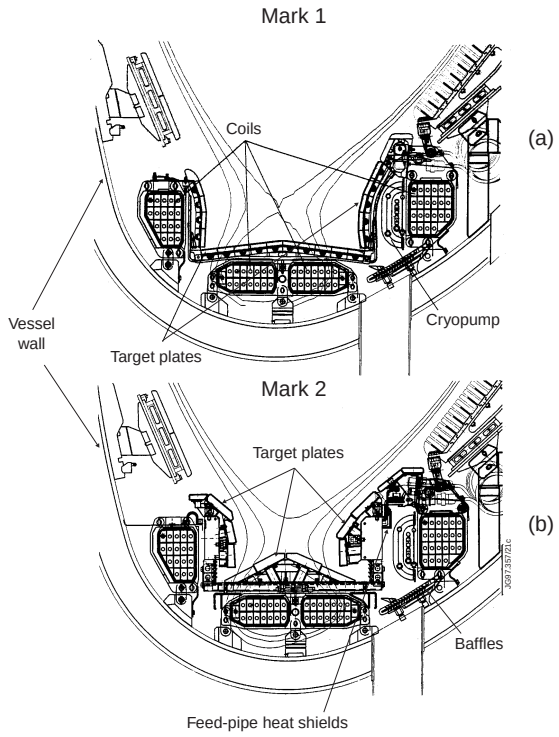

Figure 4. The JET Pumped Divertor a) MK1, b) MK2

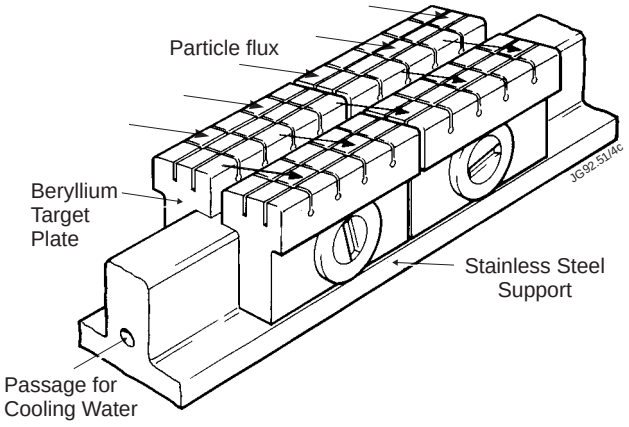

Figure 5. Three dimensional view of the MK1 target plate tiles clamped on a water cooled rode.

1.3 Target Plates (MK2 Divertor)

A second version of the divertor configuration, called MK2, (Fig 4b.) was installed in the JET torus in 1996 [19]. The MK2 Divertor has a larger surface area to which the plasma power is

conducted and therefore experiences smaller thermal gradients, than its predecessor. The installation of MK2, as well as the use of different tile materials in MK1 were implemented in order to examine the effect on plasma performance.

The MK2 configuration (Fig 4b) comprises a rigid floor and a sideways structure, continuous in the toroidal direction, and divided in 24 units, cooled in a parallel arrangement. Tile carriers and CFC tiles are accommodated in the above structure.

In addition, the outer side plate, next to the cryopump, features 48 feed pipes (two per module), as well as a set of radiation shields at the top of the pump. Instead of the 10 cm wide poloidal gaps of its predecessor the MK2 Divertor comprises the louvre, an open structure, which allows the flow of the plasma particles into the cryopump area. (The global pumping performance of the whole divertor is similar to MK1 [20]).

2 COMBINED CONDUCTION RADIATION AND CONVECTION HEAT TRANSFER

For a transient situation, an energy balance over a finite volume with mass, *m*, specific heat capacity, c_p, and temperature, T, is given by the following equation:

$$m\, C_p\, \partial T/\partial t = -\nabla q + \Phi \qquad (1)$$

The terms on the right are the thermal flux vector and the net heat generation (source term), respectively. For $\Phi=0$ (as in the case of the relevant in vessel components) the above equation shows that the total enthalpy change of a volume with respect to time, t, is equal to the gradient of the incident thermal flux, ∇q. The latter can incorporate all the basic heat transfer modes simultaneously and thus equation (1) if applied to a component *i* becomes:

$$m_i C_{pi}\, \partial T_i/\partial t = \{(\lambda_j/s_{ji})(T_j - T_i)\, dA_j\} +$$
$$+\{h_\alpha (T_i - T_f) dA_i\} + \{\sigma \varepsilon_i \varepsilon_j \varphi_{ij} (T_j^4 - T_i^4) dA_i\} +$$
$$+\{\Delta H - m' C_v' \partial T'/\partial t\} \qquad (2)$$

with,

i = component under investigation
j = surrounding component
λ = thermal conductivity
s_{ji} = conduction distance between components j, i.
A = area
h_α = heat transfer coefficient of ingress medium
T_f= temperature of ingress medium
σ= Stefan-Boltzman constant
ε = emissivity
φ_{ij} = view factor between *i* and *j* components

m' = coolant mass flow rate

C_v' = specific heat capacity of coolant

T' = temperature of coolant

ΔH = entalpy difference of coolant

The coolant's enthalpy difference ΔH is given by the following formula:

$$\Delta H = \dot{m} C_p' (T_{in} - T_{out}) \quad (3)$$

with $\dot{m}$ the coolant mass flow rate, C_p' its specific heat capacity under constant pressure and T_{in}, T_{out} the inlet and outlet temperature respectively.

The first three terms on the RHS of Eq. (2) denote conduction, convection, radiation heat transfer as derived by Fourier's, Newton's and Planck's law, respectively. The fourth term represents the rate of heat transfer from i^{th} component to the coolant. The second part of this term, $\dot{m} C_v' \partial T'/\partial t$, denotes the internal energy of the fluid. If the running medium is in the gaseous stage this term can be ignored without incorporating significant errors in the analysis (typically this term corresponds to less than 1% of the incident heat fluxes).

The heat transfer coefficient of the ingress medium, h_α, was determined by the natural convection formulae. The evaluation of the view factors φ_{ij} in Eq. 3 was carried out by means of the Hottel's Cross String method [21] as the required integration over the involved finite areas is rather complicated. The emissivity of Siclanic was measured, by means of a Dornier Selectometer appliance, while the emissivity of Graphite and Beryllium tiles was derived from [22].

The aim of the analysis is to calculate the temperature of component, *i*, at any time, *t*. With known heat fluxes and coolant temperatures, the above equation can be easily solved. However, if the outlet coolant temperature is unknown (as in most cases), an additional equation must be used. The additional equation can be derived by regarding the component *i* as a heat exchanger and if the running fluid is gas Eqs (2) & (3) yield

$$\dot{m} C_p' (T_{out} - T_{in}) = KA \, \Delta\theta_m \quad (4)$$

with,

KA = overall heat exchanger coefficient which quantifies the thermal resistance along the heat path

$\Delta\theta_m$ = mean temperature difference of a heat exchanger

The heat transfer coefficient of the coolant (incorporated in the KA term) was obtained by the respective forced convection correlations.

When there is no coolant in the i^{th} component then the fourth term on the RHS of Eq. (2) becomes zero and the general differential equation reduces accordingly. However, for a loss of flow event only the enthalpy difference term reduces to zero.

Therefore if the heat fluxes are known, the temperature of the i^{th} component can be easily found from Eqs. (1)-(4). The problem becomes more complicated when the temperatures of the

components (and thus their associated heat fluxes), are not stable but change in a transient way. It is then necessary to determine the temperature variation of all the components involved, at the same time. Integration of the above set of equations for every component of concern then results in a system of at least 18 coupled non-linear differential equations.

3. NUMERICAL ANALYSIS

A flexible, multiply lumped model based on the finite difference method was used for a series of safety analyses, during all Tokamak operating modes and under a variety of boundary conditions [23-25].

The computer code takes into account the following components: the cryopump, the divertor coil with its 11 radiation shields, the target plates and target shields, the baffles and the vacuum vessel. It deals with the as-made geometry of the whole assembly, the vacuum conditions and the coolant flow conditions for each component.

The set of the differential equations was solved by employing a finite difference method using an explicit approach. The derivative $\frac{dT}{dt}$ is approximated over a time step Δt by:

$$\frac{dT}{dt} = \frac{T(t + \Delta t) - T(t)}{\Delta t} \tag{5}$$

Thus, the problem domain (i.e., the time period of a transient) is discretized, and the values of the unknown dependent variables (temperature) are calculated only at a finite number of nodal points (i.e. the nodes are the two ends of every Δt period) instead of every point over the time domain. The geometric complexity of the problem is incorporated via the view factors in Eq. (3). Discretizing Eqs. (2) and (4) and assuming gas flow during a transient yields the following algebraic expressions.

$$m_i c_{pi} \frac{T_i(t + \Delta t) - T_i(t)}{\Delta t} = \pm\sum W_i + \dot{m} C_p' (T_{in} - T_{out})\Big|_{t=t+\Delta t} -$$

$$- m' C_v' \frac{T_i(t + \Delta t) - T_i(t)}{\Delta t} \tag{6}$$

$$\dot{m} C_p' (T_{out} - T_{in})\Big|_{t=t+\Delta t} = KA \Delta\theta_m \tag{7}$$

where, $\pm\sum W_i$ represents the first three terms of the RHS of Eq. (2), while $T_i(t)$, $T'(t)$, $T_i(t+\Delta t)$ $T'(t+\Delta t)$ are the temperatures of the i^{th} component and coolant respectively at times, t, and $t+\Delta t$.

Eqs (6)-(7) are solved in a step by step approach. The code first calculates the steady state temperatures of the concerned components by putting $dT_i=0$ in Eq. (2). The equilibrium temperatures are then the input for the transient analysis at time $t=0$. The explicitly calculated

component temperature at time t then becomes the input value for the next time step integration, between t and $t+\Delta t$. Note that the time step, Δt must be small enough to ensure that numerical instabilities are avoided. To investigate the accuracy of the numerical method employed the code was modified to incorporate the implicit approach as well. The difference between the results from both methods however is less than ±5% (average) with the explicit method being the more conservative. Typically 1200 time steps are required which takes less than 300 seconds of CPU time on an PC with a 486 processor.

The model was extensively validated by an experimental campaign focused primarily on the transient behaviour of the divertor cryopump [17], [23-25], but also extended to its associated components. This paper is focused on the studies related to the aforementioned water cooled components, namely simulations of real loss of flow events, cool downs with gaseous mediums, as well as hypothetical abnormal events, such as loss of water flow in one or both systems, loss of cryogen flow in the cryopump, loss of torus vacuum and combinations.

4 EXPERIMENTS AND ANALYSES

4.1 Cool down of baffles with Gaseous Nitrogen.

Water can be safely introduced in the baffles only if their temperature is lower than the boiling point of the cooling water, at the working pressure (otherwise steam is generated causing high thermal stresses over the relevant pipework [26]). The vessel temperature can be as high as 350^{o}C and since it is time consuming to cool it down to even 100^{o}C, (the optimum cooling rate is 20^{o}C/hr), it is necessary to employ a process which would allow a safe water insertion but under high vessel temperatures.

One approach is to start cooling the baffles with ambient *gas*, instead of water, to an adequately low temperature so that after switching to water (~5 min interval) the bulk component temperature would still stay below a safe limit (i.e.100^{o}C). Gaseous Nitrogen (GN) is chosen for the initial cool down phase because it is cheap and readily available from the JET cryoplant.

To investigate the effect of GN on the coding rate of the cryobaffles one octant was cooled with ~6.5 g/s ambient GN under good vacuum conditions (ie p~10^{-7} mbar) and relatively high vessel temperatures. The whole process has also been simulated with the model and it was shown (Fig. 6) that the baffle cools down to ~110^{o}C (i.e. > 100^{o}C) in ~3600 s with the vessel at 220^{o}C. The comparison with the experiment is good.

The same experiment was repeated at a lower vessel temperature (190^{o}C instead of 220^{o}C). The model simulation and the experimental results are shown in Figure 7. Although, the model predicts somewhat higher temperatures (conservative) the cool down time constant (3300 s) and the (final) steady-state temperature (92^{o}C) are in a good agreement with the measured ones. The cool down process appears adequate (although marginal) because taking into account the 5 min interval needed to switch from GN to water the baffle temperature will rise to 101^{o}C (i.e. just

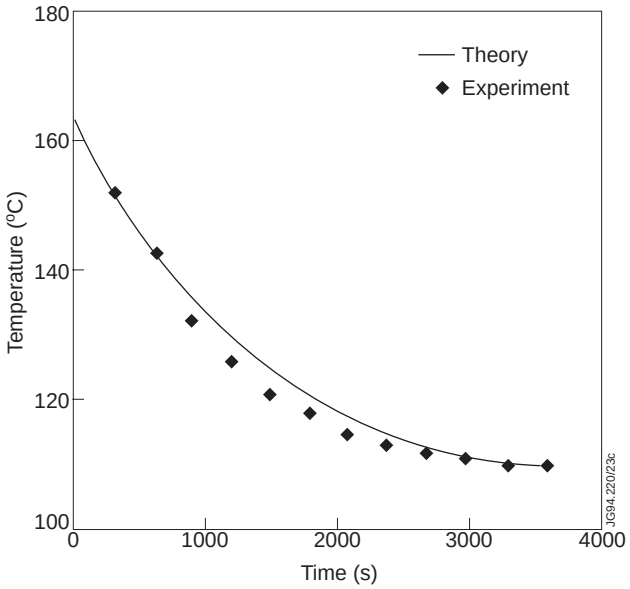

Figure 6. Correlation between experimental and theoretical exit temperature of gaseous nitrogen during a baffle cool down process with the vessel at 220°C.

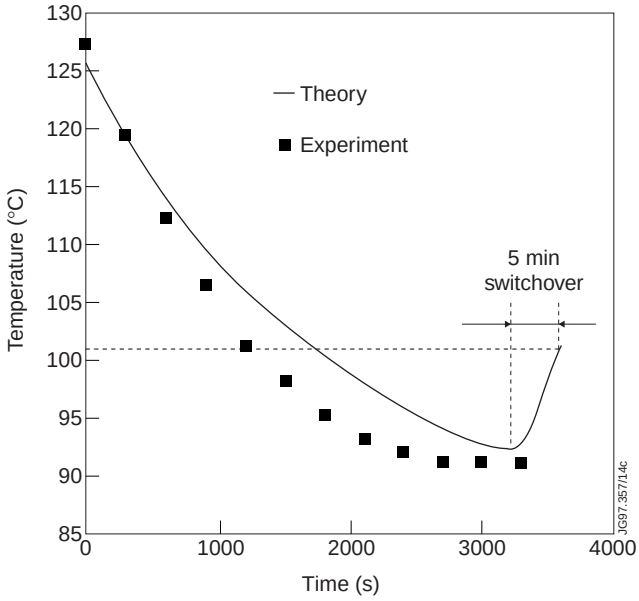

Figure 7. Comparison between experimental and theoretical exit temperature of gaseous nitrogen during a baffle cool down process with the vessel at 190°C.

above the allowable value). A sensitivity analysis with regard to the vessel temperature was performed. It was found that when the vessel is at 170°C, the final baffle temperature just prior to water insertion would be 80°C (a generous safety margin) after 3350 seconds.

4.2 CFC tile temperature measurements.

An element of concern in the MK1 Divertor was the clamping force between the tiles and the water cooled support armours (Fig 5), which affects the heat transmission between them and hence their temperature. The unknown is the steady-state tile temperature when the support structure is cold, ~20°C (i.e., cooling water is flowing in the target plates), under different vessel temperatures and good torus vacuum conditions. Tile temperature measurements were recorded with the vessel at 250°C [27]. The model performed a steady-state analysis and the comparison between the calculated and measured data as well as the extrapolation to higher vessel temperatures is illustrated in Figure 8. (High clamping force means thermal contact resistance of 180 W/m^2/degree, where the area is the contact area. For the Low Clamping force case the above value is reduced by a factor of two [27]).

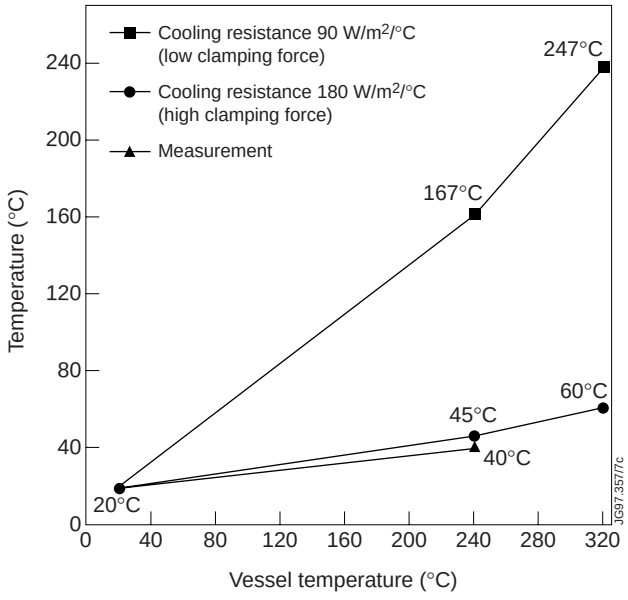

Figure 8. The effect of the clamping force on the MK1 tile temperature, with water flowing in the target plates, under good vacuum conditions.

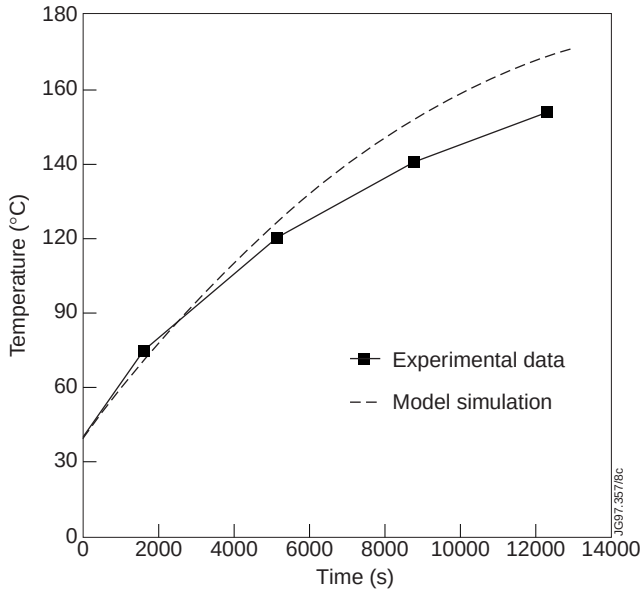

Figure 9. Correlation between the predicted and measured target plate temperature evolution of MK1, after a loss of water flow, good vacuum and vessel temperature at 523K (250^{o}C). CFC tiles on the target plates.

4.3 Radiation warm-up of the MK1 target plates with CFC tiles

A loss of water flow incident in the MK1 Divertor target plates occurred in 27/6/1994 and was recorded by the JET data acquisition systems. The torus vacuum was good ($p<10^{-6}$ mbar) and the vessel temperature was 250^{o}C. The model simulated the above incident and the comparison of the theoretical against the experimental results are demonstrated in Figure 9. The agreement with the recorded data is reasonably good.

5 DETERMINATION OF BOILING & FREEZING RISKS

5.1 Baffle Boiling risks

With relatively high vessel temperatures, the baffles are at risk of boiling in a case of loss of water flow accident. Figure 10 illustrates the calculated baffle boiling time constant (9600 s) under good torus vacuum, with LN in the cryopump, loss of water flow in the target plates and with the vessel at 250 ^{o}C. A sample of transient boiling time constants of the baffles, operating with the MK1 Divertor under different boundary conditions, is given in Table 1.

The value of 10^{3} mbar, in Table 1, is the highest possible pressure level which could be encountered inside the torus, as the protective bursting disc of the Torus is set to 50 mbar

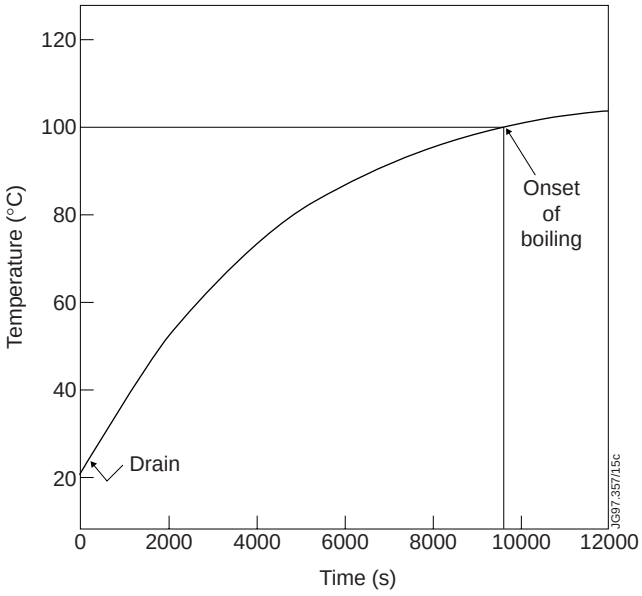

Figure 10. Baffle boiling risk, after loss of water flow in the system, good torus vacuum the cryopump cold and the vessel at 250^{o}C.

Torus Pressure [mbar]	Water Flow in Target Plates	Cryopump Condition	Baffle Boiling Time [s]
10^{3}	No	Warming up	**1550**
$>10^{-3}$	No	Warming up	**8950**
$>10^{-3}$	No	Cold 77K	**9600**
$>10^{-3}$	No	Warm 340 K	**2700**
10^{3}	No	Warm 340 K	**550**
10^{3}	Yes	Warming up	**1000**
$>10^{-3}$	Yes	Warming up	**9200**
$>10^{-3}$	Yes	Cold 77 K	**10400**
$>10^{-3}$	Yes	Warm 340 K	**2800**

Table 1: Baffle boiling time constants under different boundary conditions, and the vessel at 250°C.

(gauge). The ingressed medium is assumed to be dry air at the average temperature of the vessel. For pressures lower than 10^{-3} mbar the dominant heat transfer mode is radiation for the geometry involved [17], [24] and the vacuum is considered good (however,the JET vacuum levels are better than 10^{-7} mbar during normal operation). The cryopump is considered to be either full or empty of cryogens (at equilibrium) or undergoing a simultaneous loss of cryogen flow (transient). It is clear from Table 1 that the shortest boiling time constants (eg, 550 s) occur under bad vacuum conditions. This is an expected result and is due to the high convective heat from the hot air inside the torus. With the vessel at 320°C the above time constants reduce by an average of almost 50%.

5.2 Baffle freeze-up risks.

Under good vacuum conditions, the baffles are at risk of freezing if a loss of water flow occurs and the vessel is at relatively low temperatures. This is due to the low emissivity shiny vessel wall (ε~0.15) which cannot offer a thermal protection to the baffles from the cold blackened chevrons of the cryopump (ε~0.8).

5.2.1. Baffles in the MK1 Divertor

Figure 11 shows the maximum predicted difference between the steady-state and the transient temperature of the baffles, plotted against the vessel temperature, when there is loss of water flow, the cryopump is cold and the torus vacuum is good. It can be seen that

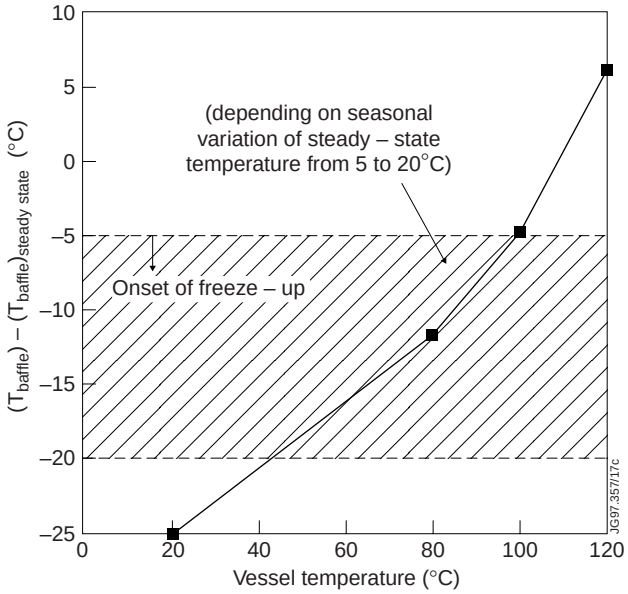

Figure 11. Baffle freeze-up risk, versus vessel temperature in loss of water flow cases.

no freeze-up risk is possible when the vacuum vessel temperature is > 100^{o}C. JET did not plan any tokamak operation with vessel temperatures lower than 250^{o}C, during the experimental campaign with the MK1.

If the torus pressure exceeds 10^{-3} mbar (due to an inleak) the above limit is relaxed, and the risk is reversed to boiling, since the ingressed medium will only add heat to the baffles, see Table 1.

5.2.2. Baffles in the MK2 Divertor

While the baffle boiling time constants are not affected by the installation of the MK2 Divertor, freeze-up risks must be re-assesed, mainly because operation with low vessel temperatures (150^{o}C) was foreseen with the new configuration. The analysis was further extended to room temperature.

The freeze-up time constants following a loss of water flow in the baffles, with vessel pressures lower than 10^{-3} mbar are shown in Table 2.

T_{vessel} [° C]	Freezing Time Constant
70	29600
60	12800
50	9200
30	6400
20	5900
10	5200

***Table 2**. Baffle freeze-up time constants versus vessel temperature, after loss of water flow, good vacuum, and with the pump cold*

The full freeze up process must take into account the latent heat of the water [25], [28]. In this case the worst time constant is relaxed from 5200 s to 6600 s. Nevertheless, the present analyses consider only the onset of a phase change (freezing or boiling) in order to obtain adequate safety margins.

If the torus pressure increases to a range higher than a few mbar (and up to 1 bar), viscous flow prevails [17], [24] and the heat flux to the baffles starts to increase. Under these circumstances the freeze up risk diminishes even with the vessel at its lowest (room) temperature (20^{o}C). For pressures between 10^{-3} mbar and 1 mbar, there exist molecular or transitional flow regimes, determined by the molecular mean free path of the inleak. Studies regarding this pressure regime are beyond the scope of this paper, but it has been found that if there are any freeze-up phenomena they will be slower than those given in Table 2.

5.3 Target Plates (MK1 Divertor)

The MK1 Divertor contains a set of water cooled shields, situated at the rear side of each of the 48 target plate modules and only 10 mm away from the cryopump (Fig 3, 12). These shields have a relatively low mass and are in danger of boiling or freezing should there be a loss of water there (the shields are cooled in parallel with the target plates).

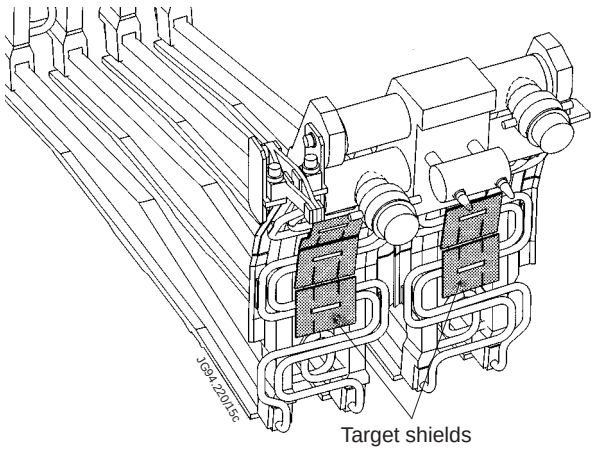

Figure 12. Isometric view of the MK1 target shields attached on a target plate module.

Under good vacuum conditions, the target shields are at risk of boiling, should there be a loss of water flow. The boiling risk increases if a simultaneous loss of cryogen flow occurs, or if the cryopump is empty of coolants. The shortest boiling time constants are ~5800 s and ~10500 s with CFC and beryllium tiles respectively. The fact that boiling occurs much faster with CFC tiles on the Divertor is due to their emissivity (ε ~0.9), which is much higher than that of the beryllium tiles (ε ~0.15-0.3) [22].

At the other extreme, when there is loss of water flow in the target plates and a simultaneous loss of torus vacuum, the risk may be of a freeze-up.

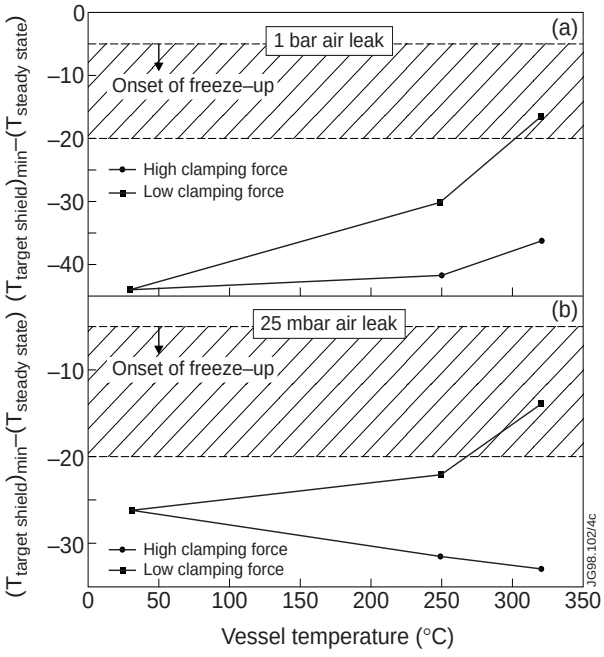

Figure 13. MK1 target shield freeze-up risk, versus vessel temperature, with a) 1 bar and b) 25 mbar air leak, CFC tiles on the target plates and different clamping force.

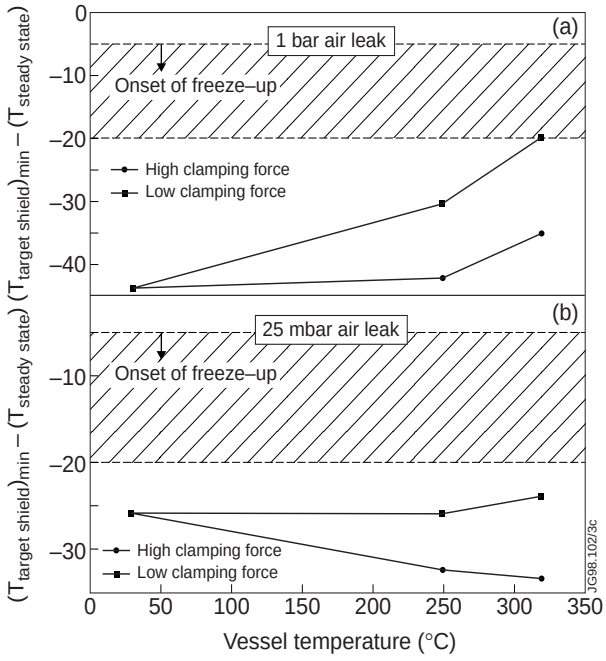

Figure 14. MK1 target shield freeze-up risk, versus vessel temperature, with a) 1 bar and b) 25 mbar air leak, beryllium tiles on the target plates and different clamping force.

Figures 13, 14 illustrate the predicted freeze-up risk of the target shields at different boundary conditions, accounting for the effect of tile material (ie beryllium or CFC), and clamping force. The analysis predicts that freeze-up is inevitable, except when the vessel temperature is very high (ie > 280^{o}C). The effect of tile material is the same as in the case of good vacuum. Furthermore, if the clamping force is high (the more realistic situation as illustrated in Fig.8) the tiles remain relatively colder and the freeze-up risk becomes higher, while freeze-up occurs at all vessel temperatures. The shortest freeze-up time constant was found to be ~1000 s with CFC tiles and ~200 s with beryllium tiles.

5.4 Target Plates (MK2 Divertor)

The MK2 Divertor (Fig 4b) comprises new components at risk namely the louvre (a baffle arrangement next to the cryopump) and part of the module feed pipework. There are no target shields in this geometry. In addition, the tiles of the MK2 Divertor have higher steady state temperatures, due to a high thermal resistance between them and the water cooled armours (4 point contacts per tile). Their temperatures are similar to the low clamping force curve (Fig 8), [27]. Therefore the MK2 tiles are significantly hotter than their counterparts in MK1 and different boiling and freeze-up risks were expected.

5.4.1. Boiling and Freeze-up Risks of MK2 Louvre and Feed Pipework

The louvre is at risk of boiling should there be a loss of water flow, with the vessel temperature ≥220^{o}C, and regardless of the vacuum conditions. This is mainly due to the high heat flux from the hot CFC tiles (positive net thermal balance). A sample of calculated boiling time constants with the vessel at 250^{o}C and different boundary conditions is given in Table 3. However, with low (<80^{o}C) vessel temperatures (thus low tile temperatures), and bad vacuum conditions, the risk is reversed to a freeze-up (time constant: ≥ 5500 s).

As far as the feed pipework is concerned, significant freeze-up risks may occur even at elevated vessel temperatures, as can be seen in Table 3.

Cryopump Condition	**Torus Pressure [mbar]**	**Louvre Boiling Time Constant [s]**	**Feed-pipe Freeze-up Time Constant [s]**	**Freeze-up Time Const. with Electr. Isolated Shield**
Cold 77 K	$>10^{-3}$	1360	5840	27800
Cold 77 K	10^{3}	700	660	>>2440
Warming up	$>10^{-3}$	1200	13600	No risk
Warming up	10^{3}	600	800	>>3900
Empty	$>10^{-3}$	960	No risk	No risk
Empty	10^{3}	350	No risk	No risk

Table 3: Conditions leading to a boiling risk of the water cooled louvre and feed pipe, with vessel at 250°C.

Further analysis showed that by installing a single heat shield, between the feed pipe and the cryopump, freeze-up risks would be greatly reduced or even eliminated. The effect of a radiation shield on the freeze-up time constants of the feed pipe is also shown in Table 3. Due to the substantial protection against freezing, 48 stainless steel heat shields (one per pipe) were implemented in the target plate structure prior to its installation (1996), see Fig 4b.

6 TARGET PLATE WATER REFILLING (MK2 DIVERTOR)

The criteria for safe water introduction in the target plates are the same as those adopted for the refilling of baffles (section 3.1). The water cooling circuit of the MK2 target plates is shown in Figure 15 (a). Every target plate module (24 in total) accommodates the feed pipework (an inlet and an outlet pipe). The pipes (i.e. 48 in total) are mounted to a pair of "French horns" (expansion loops), which are interconnected by a bleed pipe.

The French horns (Fig 15b) are attached to two horizontal manifolds and their purpose is to accommodate the differential expansion between the upper and lower part of the target plate cooling circuit. (The upper part is connected to the normally hot vessel, while the lower part is attached to the relatively cold divertor coils, which are kept at temperatures lower than 80^{o}C). The coolant exits the circuit via the long vertical tube. The above circuit is illustrated in Figure 15 (b).

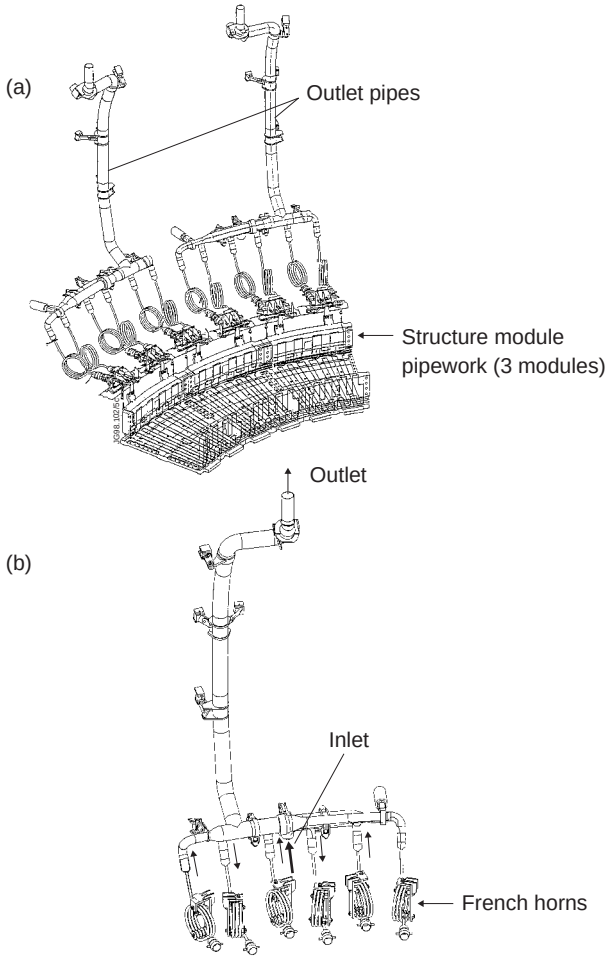

Figure 15. a) the cooling circuit of a MK2 target plate section (3 modules) (b) the in- vessel pipework above 1.5 target plate modules.

After a loss of water flow in the target plates, the stagnant medium is drained out within the predicted boiling or freeze-up time constants (see Section 5). It is required to know the time within which the water flow can be safely reinstated, under high vessel temperatures. Refilling should be done so that every part of the relevant structure remains at temperatures below 100^{o}C, to prevent boiling of the incoming water and subsequent high thermal stresses [26].

The in-vessel part of the target plate cooling circuit (Figure 15) can be divided in two main subsystems: the target plate modules and the pipework above them. It is assumed that when water is flowing the temperature of the system is 20^{o}C everywhere. However, in a loss of flow

accident the modules heat up very slowly compared to the rest of the pipework, due to their high thermal mass. It was found that the target plate warm-up rate is 1°C/min, during gas cooling with the vessel at 320°C, [27].

6.1 Direct refilling without gas cooling

The refilling process of the MK2 target plate structure was simulated under a set of different boundary conditions. Initially only the French horns were considered because they have the lower thermal mass and hence the faster warm-up.

With the vessel at 320°C and under black body radiation conditions (the French horn is a small pipe enclosed by large vacuum vessel) and without any cooling (i.e. the stagnant water is assumed drained, after a possible loss of water flow), a dry French horn pipe reaches 100°C in ~5 min (Fig 16).

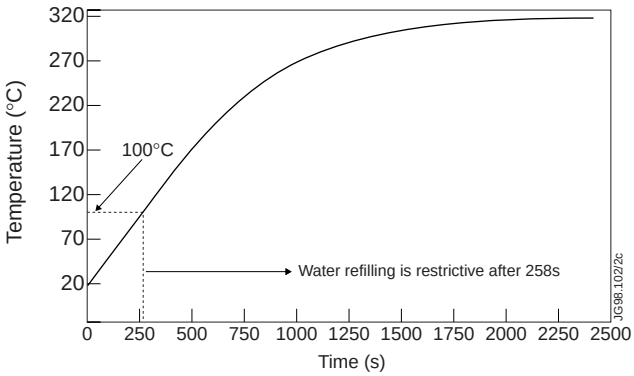

Figure 16. Transient warm-up of a dry French horn of the MK2 Divertor cooling circuit, under good torus vacuum and the vessel at 320°C.

6.2 Refilling with gas cooling

The above short time constant (5 min) can be increased by employing gas cooling prior to water introduction. The assumptions adopted for this particular analysis were that refilling takes place under good torus vacuum, GN can be readily introduced after a loss of water flow, at 4 bar and a flow rate per French Horn is between 5.2-10.4 g/s. Additionally, it was assumed that with the vessel at 320°C, the warm-up rate of the divertor structure would remain at 1°C/min (ie not affected by GN), [29].

The gas flow distributes itself between the divertor support structure and the French horn bypass pipes. The hottest part of the system is the exit French horn since it also comes into contact with the part of the coolant which passes through the target plate structure, the temperature of which rises continuously by 1 °C /min.

Figures 17 and 18 demonstrate the thermal behaviour of the inlet and outlet French horn respectively, with the vessel at 320° C, good vacuum conditions and different GN mass flow rates. It is clear that refilling of the target plate structure can take place even after~60 min from the initiation of a possible loss of water flow, without allowing any part of the system to reach temperatures higher than 100°C. This can be achieved even with half the assumed GN flow rate (i.e., 5.2 g/s per French horn).

Additional sensitivity analyses were performed in order to quantify the effect of different vessel temperatures, as well as delays in commencing the gas cooling process (so far it was assumed that gas is introduced immediately after the loss of water flow). Under these

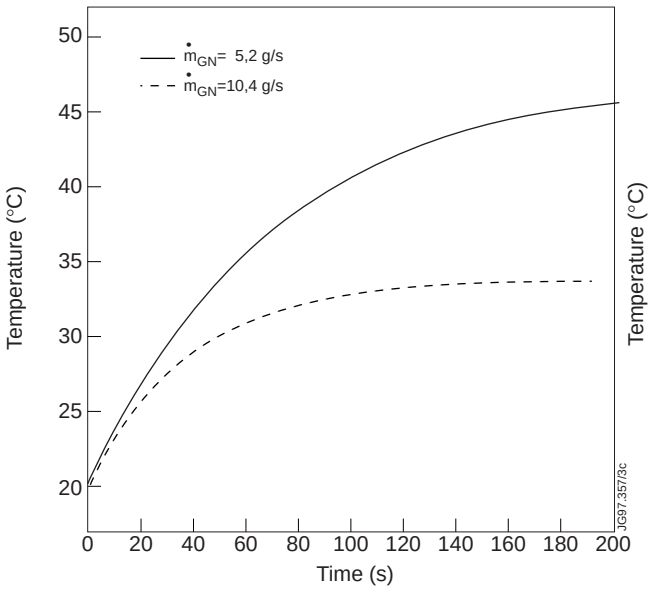

Figure 17. Transient warm-up of the inlet French horn during a gas cooling process with different mass flows, under good torus vacuum and the vessel at 320°C.

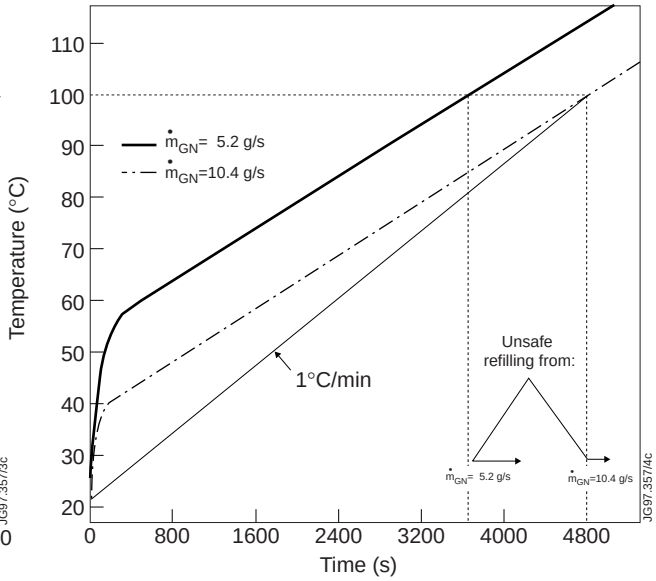

Figure 18. Transient warm-up of the outlet French horn during a gas cooling process with different mass flows, under good torus vacuum and the vessel at 320°C.

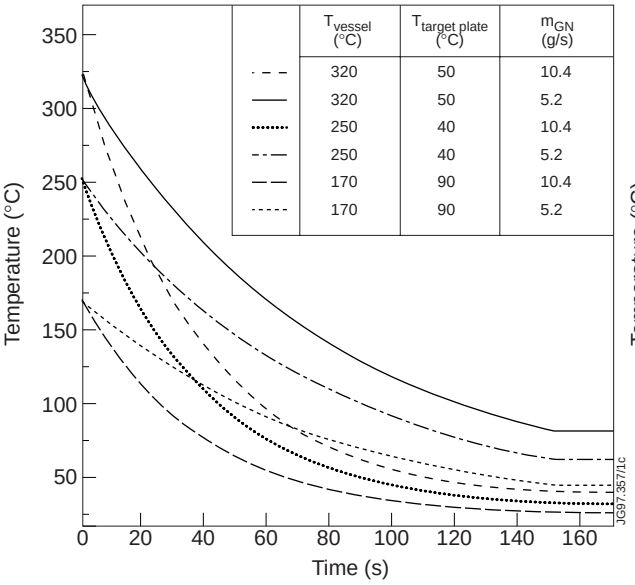

Figure 19. Temperature evolution of the inlet French horn during a gas cooling process under different boundary conditions.

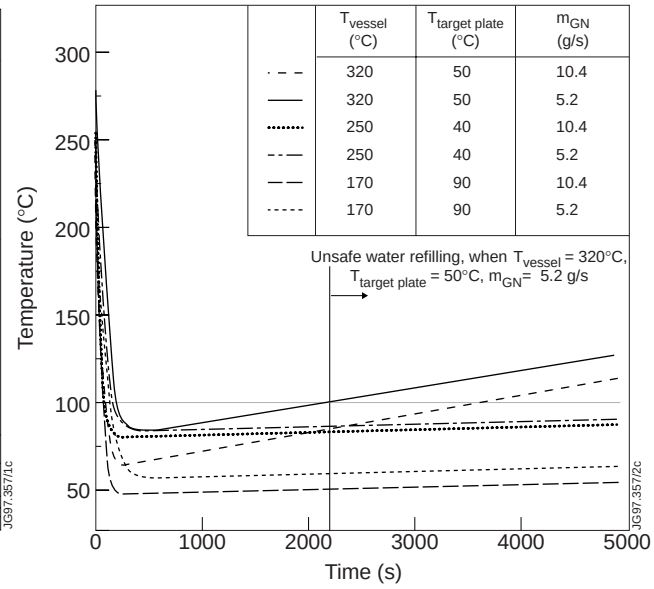

Figure 20. Temperature evolution of the outlet French horn during a gas cooling process under different boundary conditions.

conditions, the French horn can have same temperature as the vessel, ie, between 20°C (initiation) and 320°C (maximum vessel temperature).

Figures 19, 20 demonstrate the gas cooling process of the French horns under different boundary conditions. The sensitivity analyses resulted in the following results.

- With the vessel temperature at 170°C (i.e. 443K) and with the target plates at 90°C the temperature of the hottest French horn is ~80°C and therefore refilling can take place safely (flow rate 10.4 g/s).

- With the vessel temperature at 250^{o}C (i.e. 523K) refilling should take place within >130 min (flow rate 10.4 g/s, maximum temperature of the hottest French horn is 100^{o}C).
- With the vessel temperature at 320^{o}C, the gas cooling of the French horn is effective only up to ~2200 s, with 5.2 g/s flow rate.

7. THE SAFETY PROTECTION SYSTEM

The above analyses enabled the quantification of detailed boiling and freeze-up time constants under a diverse set of boundary conditions. Protective actions (like draining) have been identified within the above time limits and formed the basis of one of the JET Safety Machine Protection Systems. A typical logic diagram with deals with the protection against boiling of the target plates in case of a loss of flow accident under various conditions is illustrated in Figure 21.

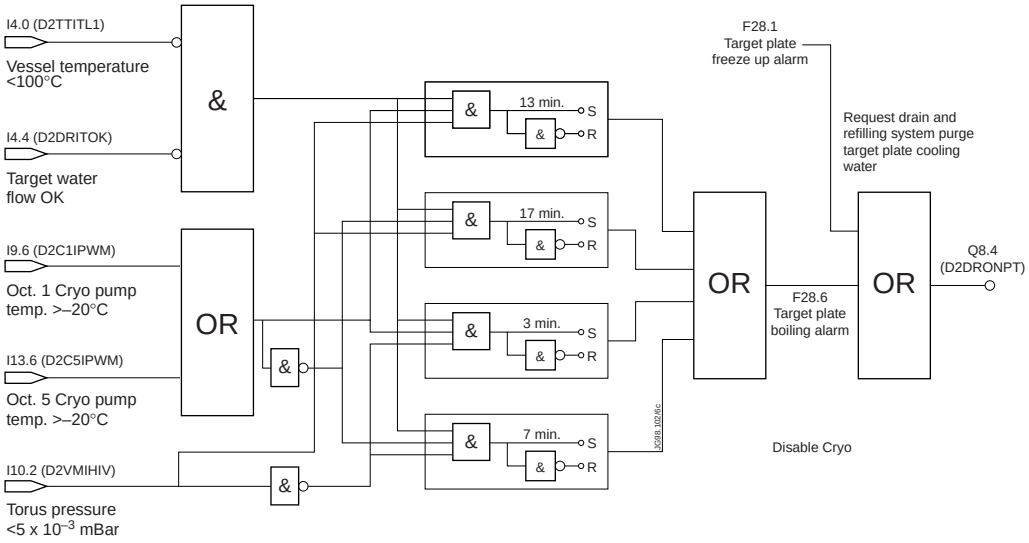

Figure 21. A typical Logic Diagram of the target plate protection against boiling during abnormal scenarios.

The fully automatic protection system operates continuously (on a 24 hr basis) and indeed reacted appropriately during a number of abnormal real events since its implementation [17], [25], [28], protecting adequately the components of concern.

8. CONCLUSIONS

A flexible mathematical code was applied to analyse the behaviour of water cooled structures inside the JET thermonuclear Tokamak. Similar modelling techniques have been employed for theoretical transient analyses of various fusion components [30]-[33].

The model simulations of normal and abnormal scenarios were supported by a number of in-vessel experiments. The model has also been extended to cryogenic components and in particular the in-vessel and the LHCD cryopumps [25], [28].

A coherent and fully automatic protection system was developed on the basis of these transient analyses and totally implemented in the JET software.

All components have been operating since 1994 without a single need for repair or in-vessel intervention.

9. ACKNOWLEDGEMENTS

The authors wish to thank Dr D Stork , Dr W Obert, Mr H Van der Beken, Dr E Deksnis for valuable comments and discussions.

REFERENCES

[1] **W Kramer**: Critical Safety Issues in the design of fusion machines, *Fusion Engineering & Design*, Vol 14, pp 49-63, North Holland, Amsterdam, 1991.

[2] **J G Crocker and D F Holland**: Safety and Environmental Issues of Fusion Reactors, *Proc. of the IEEE*, Vol. 69, No. 8, pp 968-976, August 1981.

[3] **J Raeder and W Gulden**: NET Safety Analyses & the European Safety Environmental Programme, *Fusion Engineering & Design*, Vol 11, pp 63-84, North Holland, Amsterdam, 1989

[4] **M T Porfiri et al**: ITER LOCA Sequences. Probabilistic Safety Assessment, *Proc. on the 18th Fusion Technology*, Vol. 2, pp 1465-1468, North Holland, 1994

[5] **J E. Massidda and M S Kazimi**: Thermal Design Consideration for Passive Safety of Fusion Reactors, Institute of Technology Plasma Fusion Centre, PFC/RR-87-18, Massachusetts, December 1987.

[6] **I Cook and C G Gimblett:** A risk perspective on fusion safety phenomena, *Fusion Engineering & Design*, Vol 17, pp 301-306, North Holland, Amsterdam, 1991.

[7] **E E Lewis**: Nuclear Power Reactor Safety, John Wiley & Sons, Inc., 1977.

[8] **M Iseli, H-W Bartels**: Design and Safety Criteria for Reactor Relevant Heat Transport Systems, *17th Proc. on Fusion Technology*, London, UK, pp 1668-1672, September 1992.

[9] **A C Bell, M Wright**: Analysis for the Safety Case for JET D-T Operation, *17th Proc. on Fusion Energy*, San Diego, USA, October 1997,to appear.

[10] **The JET Team (presented by D Stork):**JET Engineering Development towards D-T Operations in an ITER-like Machine Configuration, *17th Proc. on Fusion Energy*, San Diego, USA, October 1997, to appear.

[11] **J Raeder et al**: Safety Analysis & Radioactivity confinement for ITER, *Fusion Engineering & Design*, Vol 16, pp 35-43, North Holland Amsterdam, 1991.

[12] **A Bell et al**: Environmental monitoring for tritium at JET, *Proc on Fusion Technology*, Vol 28, no. 3, Part 1, 1995.

[13] **A C Bell, M Wykes and B J Green:** Safety aspects and approvals for the first tritium experiment, *Fusion Engineering & Design*, Vol. 19, No 2, pp 169-178, September 1992.

[14] **The JET Team (presented by A Tanga):** First Results with the Modified JET. Journal of *Plasma Physics & Controlled Fusion*, 1994, **36**, 39-54 (Inst. of Physics Publishing, UK).

[15] **The JET Team (presented by M Keilhacker):** JET Results with the New Pumped Divertor and Implications for ITER, Journal of *Plasma Physics & Controlled Fusion*, 1995, **37**, 3-18 (Inst. of Physics Publishing, UK).

[16] **S Papastergiou, W Obert and E Thompson**: The JET In-vessel Cryopump. Design, Manufacture, Assembly, Testing and Operational Safety,(JET Report -P(94)37, 1994.

[17] **P A Ageladarakis:** Aspects of Operational Safety & Mechanical Integrity of the Cryopump System in the JET Fusion Tokamak, *PhD Thesis* 1996, Imperial College, London.

[18] **E Bertolini for the JET Team:** JET with a Pumped Divertor: design, construction, commissioning and first operation, *Fusion Engineering & Design*, 1995, **30,** 53-66 (North Holland, Amsterdam).

[19] **H Altmann et al**: Design of the MARK II Divertor with large carbon fibre composite (CFC) tiles, Proc of the 18th Symposium on Fusion Technology, Vol. 1, pp 275-279, Germany, 1994.

[20] **R Mohanti** Personal Communication, JET, 1995.

[21] **R Siegel, J R Howell**: Thermal Radiation Heat Transfer, 1983, Chpt 7 , 202-210, (Hemisphere Publishing Corp., New York).

[22] **H D Falter et al:** High Heat Flux Exposure Tests on 10 mm Beryllium Tiles Brazed to an Actively Cooled Vapotron made from CuCrZr, JET Report, JET-R(96)02, 1996.

[23] **S Papastergiou, P Ageladarakis W Obert & E Thompson**: Operational Safety of the JET In-Vessel Divertor Cryopump System, Proc of Fusion Technology Vol 1, pp 343-346, Elsevier Science 1994.

[24] **P A Ageladarakis, S Papastergiou, N P O'Dowd, G A Webster**: Theoretical and Experimental Simulation of Accident Scenarios of JET Cryogenic Components. Part I: The JET In-Vessel Cryopump. Proc of IME, Mechanical Engineering Science, Part C, submitted.

[25] **P Ageladarakis et al:** The Model and Experimental Basis for the Design Parameters of The JET Divertor Cryopump Protection System Including Variations in Divertor Geometry and First Wall Materials, *Proc of Fusion Technology*, Vol 1, pp 431-434, North Holland, Lisbon, 1996.

[26] **P Miele**: Thermo-Stress Analysis on the MKII Cooling System, JET Technical Report, 1996.

[27] **E Desknis:** Personal Communication, JET 1995.

[28] **P A Ageladarakis, S Papastergiou, N P O'Dowd, G A Webster**: Theoretical and Experimental Simulation of Accident Scenarios of JET Cryogenic Components. Part II: The JET LHCD Cryopump. Proc of IME, Mechanical Engineering Science, Part C, submitted.

[29] **H Altmann:**Personal Communication, JET 1996.

[30] **A Y Ying, A R Raffray, and M Abdou:** Benefits of Natural Convection in Solid Breeder Blankets with Poloidal Coolant Channels under LOFA Conditions, *Fusion Engineering and Design*, 1991, **17**, 313-319.

[31] **A Y Ying, A R Raffray, and M Abdou:** LOFA Analysis for US ITER Solid Breeder Blanket, *Fusion Technology*, 1991, **19**, 1481-1486.

[32] **Z R Gorbis, et al:** LOCA Study for a Helium-Cooled Solid Breeder Design for ITER, *Fusion Technology*, 1989, **15**, 821-826.

[33] **L S Tong and J Weisman:** Thermal analysis of Pressurised Water Reactor, 2nd edition, *American Nuclear Society*, Illinois 1979,134-141.